# Set-Membership Filtering-Based Leader–Follower Synchronization of Discrete-Time Linear Multi-Agent Systems

**Diganta Bhattacharjee**
Department of Mechanical and Aerospace Engineering,
The University of Texas at Arlington,
Arlington, TX 76019
e-mail: diganta.bhattacharjee@mavs.uta.edu

**Kamesh Subbarao**
Professor
Department of Mechanical and Aerospace Engineering,
The University of Texas at Arlington,
Arlington, TX 76019
e-mail: subbarao@uta.edu

*In this paper, a set-membership filtering-based leader–follower synchronization protocol for discrete-time linear multi-agent systems is proposed, wherein the aim is to make the agents synchronize with a leader. The agents, governed by identical high-order discrete-time linear dynamics, are subject to unknown-but-bounded input disturbances. In terms of its own state information, each agent only has access to measured outputs that are corrupted with unknown-but-bounded output disturbances. Also, the initial states of the agents are unknown. To deal with all these unknowns (or uncertainties), a set-membership filter (or state estimator), having the "correction-prediction" form of a standard Kalman filter, is formulated. We consider each agent to be equipped with this filter that estimates the state of the agent and consider the agents to be able to share the state estimate information with the neighbors locally. The corrected state estimates of the agents are utilized in the local control law design for synchronization. Under appropriate conditions, the global disagreement error between the agents and the leader is shown to be bounded. An upper bound on the norm of the global disagreement error is calculated and shown to be monotonically decreasing. Finally, a simulation example is included to illustrate the effectiveness of the proposed leader–follower synchronization protocol.*
[DOI: 10.1115/1.4049553]

*Keywords: multi-agent systems, cooperative control, synchronization, set-membership filtering, optimization*

## 1 Introduction

Cooperative control of multi-agent systems can be applied to solve a number of engineering problems and has attracted much attention in the last few decades. The applications of cooperative control include distributed task assignment and consensus problems, formation flight of spacecrafts and aerial vehicles, distributed estimation problems, and so on (see, for example, Refs. [1–6]). All of these applications typically require some degree of cooperation and synchronization among the agents. In the context of synchronization (or consensus), there are several types of problems that have been investigated in the existing literature. These are (a) synchronization without a leader (see, for example, Refs. [7] and [8]), (b) leader–follower synchronization (see, for example, Refs. [9–12]), (c) average consensus (see, for example, Refs. [13] and [14]), (d) bipartite consensus (see, for example, Ref. [15]), and so on. In this paper, we focus on leader–follower synchronization in the presence of a leader that pins to a group of agents, all having high-order discrete-time linear (time-invariant) dynamics.

**1.1 Motivation.** Most of the studies in the existing literature regarding multi-agent synchronization assume perfect modeling of the system, i.e., the mathematical description of the system is assumed to be perfect (see, for example, Refs. [8,10–12,16], and [17]). However, this is incompatible with real-world engineering problems where the dynamical system is subject to unknown input disturbances, parametric uncertainties, unmodeled dynamics, etc. Because of these phenomena, the state of the system cannot be known precisely and should be considered uncertain. For an overview on synchronization in uncertain multi-agent systems, see Refs. [6,7,9], and [18] and references therein. Among the above-mentioned phenomena, we focus on unknown input disturbances in this paper. Apart from the perfect system modeling assumption, perfect information regarding the states of the agents (full-state feedback) is assumed to be available for synchronization protocol design in a large number of studies (see, for example, Refs. [8,10,16]). Again, this assumption does not hold for practical applications where measured outputs (some function of the states), subject to output disturbances, are available. Although observer-based approaches, without considering output disturbances, have been investigated in the literature (see, for example, Refs. [4,9], and [17]), a state estimation or filtering-based approach would be more suitable to address the effects of both input and output disturbances in the synchronization problem (see, for example, Ref. [5]).

The Kalman filter [19], which is one of the most widely studied stochastic filtering techniques, assumes that the input and output disturbances are Gaussian noises with known statistical properties. However, this assumption is difficult to validate in practice and might not hold for real-world systems. Therefore, it seems more realistic to assume the disturbances to be unknown-but-bounded [20,21]. This approach leads to the concept of set-membership or set-valued state estimation (or filtering) (see, for example, Refs. [20–26]), which is deterministic and more suited to several practical applications [24]. Although the set-theoretic or set-valued concepts for synchronization have been investigated in the existing literature (see, for example, Refs. [27–30]), studies explicitly utilizing set-membership or set-valued estimation techniques for the multi-agent synchronization problem are relatively rare (see, for instance, Refs. [13] and [14]), despite the practical significance of this class of estimators/filters. Recently, a leader–follower synchronization protocol using set-membership estimation techniques was put forward in Ref. [31]. The synchronization objective in Ref. [31] was to construct ellipsoids centered at the leader's state trajectory that contained states of the agents. This, however, is different from the concept of conventional leader–follower synchronization where the objective is to make the states of the agents converge to the leader's state trajectory. To the best of our knowledge, set-membership estimation techniques have not been employed for the conventional leader–follower synchronization problem in the existing literature.

**1.2 Technical Approach and Contributions.** The technical approach and contributions of the paper are summarized in the following list:

- We develop a set-membership estimation-based (conventional) leader–follower synchronization protocol for high-order discrete-time linear multi-agent systems with the agents subject to unknown-but-bounded input and output disturbances. To the best of our knowledge, this is a novel contribution.
- Specifically, we focus on the ellipsoidal state estimation problem and adopt the terminology set-membership filter

Contributed by the Dynamic Systems Division of ASME for publication in the Journal of Dynamic Systems, Measurement, and Control. Manuscript received July 1, 2020; final manuscript received December 14, 2020; published online February 4, 2021. Assoc. Editor: Luca Consolini.

(SMF). Based on the approaches given in Refs. [23–26], we convert the set estimation problem into a recursive algorithm that requires solutions to two semidefinite programs (SDPs) at each time-step.

- We consider each agent to be equipped with the SMF that estimates the state of the agent. Further, we assume that the agents are able to share the state estimate information with the neighbors locally and that information is utilized in the local control synthesis for synchronization. The local controller for each agent is chosen based on an $H_2$ type Riccati-based approach [16]. We show that the global error system is input-to-state stable (ISS) with respect to the input disturbances and estimation errors. Sufficient conditions for input-to-state stability are provided in terms of the system matrices of the agents, the Riccati design, and the interaction graph.
- Further, we calculate an upper bound on the norm of the global disagreement error and show that it decreases monotonically, converging to a limit as time goes to infinity.

The rest of this paper is organized as follows. Section 2 describes the preliminaries required for the SMF design. The formulation of the SMF is given in Sec. 3. The control input synthesis and related results for synchronization are given in Sec. 4. Finally, Sec. 5 includes the simulation example, and Sec. 6 presents the concluding remarks.

*Notations and Definitions.* The symbol $\mathbb{Z}_\star$ denotes the set of non-negative integers. For a square matrix $\boldsymbol{X}$, the notation $\boldsymbol{X} > 0$ (respectively, $\boldsymbol{X} \geq 0$) means $\boldsymbol{X}$ is symmetric and positive definite (respectively, positive semidefinite). Similarly, $\boldsymbol{X} < 0$ (respectively, $\boldsymbol{X} \leq 0$) means $\boldsymbol{X}$ is symmetric and negative definite (respectively, negative semidefinite). Furthermore, $\rho(\boldsymbol{X})$ denotes the spectral radius of a square matrix $\boldsymbol{X}$. For any matrix $\boldsymbol{Y}$, $\sigma_{\max}(\boldsymbol{Y})$ stands for the maximum singular value of $\boldsymbol{Y}$. $C(a, b)$ denotes an open circle of radius $b$ in the complex plane, centered at $a \in \mathbb{R}$. Notations $\mathrm{diag}(\cdot)$, $\boldsymbol{I}_n$, $\boldsymbol{O}_n$, $1_n$, and $0_n$ denote block-diagonal matrices, the $n \times n$ identity matrix, the $n \times n$ null matrix, and the vector of ones and zeros of dimension $n$, respectively. For vectors $\boldsymbol{x}_1, \boldsymbol{x}_2, \ldots, \boldsymbol{x}_M$, we have $\mathrm{col}[\boldsymbol{x}_1, \boldsymbol{x}_2, \ldots, \boldsymbol{x}_M] = [\boldsymbol{x}_1^{\mathrm{T}}\, \boldsymbol{x}_2^{\mathrm{T}} \ldots \boldsymbol{x}_M^{\mathrm{T}}]^{\mathrm{T}}$. The symbol $|\cdot|$ denotes standard Euclidean norm for vectors and induced matrix norm for matrices. For any function $\boldsymbol{\theta}\colon \mathbb{Z}_\star \to \mathbb{R}^n$, we have $||\boldsymbol{\theta}|| = \sup\{|\boldsymbol{\theta}_k| \colon k \in \mathbb{Z}_\star\}$. This is the standard $l_\infty$ norm for a bounded $\boldsymbol{\theta}$. Ellipsoids are denoted by $\mathcal{E}(\boldsymbol{c}, \boldsymbol{P}) = \{\boldsymbol{x} \in \mathbb{R}^n \colon (\boldsymbol{x} - \boldsymbol{c})^{\mathrm{T}} \boldsymbol{P}^{-1} (\boldsymbol{x} - \boldsymbol{c}) \leq 1\}$, where $\boldsymbol{c} \in \mathbb{R}^n$ is the center of the ellipsoid and $\boldsymbol{P} > 0$ is the shape matrix that characterizes the orientation and "size" of the ellipsoid in $\mathbb{R}^n$. Notations $\mathrm{trace}(\cdot)$ and $\mathrm{rank}(\cdot)$ denote trace and rank of a matrix, respectively, and $\otimes$ denotes the Kronecker product. The superscript T means vector or matrix transpose.

Definition 1 [32,33]. *A function $\gamma\colon \mathbb{R}_{\geq 0} \to \mathbb{R}_{\geq 0}$ is a class $\mathcal{K}$ function if it is continuous, strictly increasing and $\gamma(0) = 0$. A function $\beta\colon \mathbb{R}_{\geq 0} \times \mathbb{R}_{\geq 0} \to \mathbb{R}_{\geq 0}$ is a class $\mathcal{KL}$ function if, for each fixed $t \geq 0$, the function $\beta(\cdot, t)$ is a class $\mathcal{K}$ function and for each fixed $s \geq 0$, the function $\beta(s, \cdot)$ is decreasing and $\beta(s, t) \to 0$ as $t \to \infty$.*

## 2 Preliminaries

Consider the discrete-time dynamical systems of the form

$$\begin{aligned} \boldsymbol{x}_{k+1} &= \boldsymbol{A}\boldsymbol{x}_k + \boldsymbol{B}\boldsymbol{u}_k + \boldsymbol{G}\boldsymbol{w}_k \\ \boldsymbol{y}_k &= \boldsymbol{C}\boldsymbol{x}_k + \boldsymbol{D}\boldsymbol{v}_k, \quad k \in \mathbb{Z}_\star \end{aligned} \tag{1}$$

where $\boldsymbol{x}_k \in \mathbb{R}^{\bar{n}}$ is the state, $\boldsymbol{u}_k \in \mathbb{R}^{\bar{m}}$ is the control input, $\boldsymbol{w}_k \in \mathbb{R}^{\bar{w}}$ is the input disturbance, $\boldsymbol{y}_k \in \mathbb{R}^{\bar{p}}$ is the measured output, and $\boldsymbol{v}_k \in \mathbb{R}^{\bar{v}}$ is the output disturbance. Also, $\boldsymbol{A}$, $\boldsymbol{B}$, $\boldsymbol{G}$, $\boldsymbol{C}$, and $\boldsymbol{D}$ are system matrices of appropriate dimensions. Following are the assumptions for systems of the form given in Eq. (1).

Assumption 1.

*(1.1) The initial state $\boldsymbol{x}_0$ is unknown. However, it satisfies $\boldsymbol{x}_0 \in \mathcal{E}(\hat{\boldsymbol{x}}_0, \boldsymbol{P}_0)$, where $\hat{\boldsymbol{x}}_0$ is a given initial estimate and $\boldsymbol{P}_0$ is known.*

*(1.2) $\boldsymbol{w}_k$ and $\boldsymbol{v}_k$ are unknown-but-bounded for all $k \in \mathbb{Z}_\star$. Also, $\boldsymbol{w}_k \in \mathcal{E}(0_{\bar{w}}, \boldsymbol{Q}_k)$ and $\boldsymbol{v}_k \in \mathcal{E}(0_{\bar{v}}, \boldsymbol{R}_k)$ for all $k \in \mathbb{Z}_\star$, where $\boldsymbol{Q}_k$, $\boldsymbol{R}_k$ are known.*

We intend to develop an SMF for systems of the form in Eq. (1), having a correction-prediction structure similar to the Kalman filter variants (see, for example, Ref. [19]). Note that the SMF design in this paper is motivated by the SMF developed by the authors in Ref. [34]. The filtering objectives are as follows, where the corrected and predicted state estimates at time-step $k$ are denoted by $\hat{\boldsymbol{x}}_{k|k}$ and $\hat{\boldsymbol{x}}_{k+1|k}$, respectively [34].

### 2.1 Correction Step.

At each time-step $k \in \mathbb{Z}_\star$, upon receiving the measured output $\boldsymbol{y}_k$ with $\boldsymbol{v}_k \in \mathcal{E}(0_{\bar{v}}, \boldsymbol{R}_k)$ and given $\boldsymbol{x}_k \in \mathcal{E}(\hat{\boldsymbol{x}}_{k|k-1}, \boldsymbol{P}_{k|k-1})$, the objective is to find the optimal correction ellipsoid, characterized by $\hat{\boldsymbol{x}}_{k|k}$ and $\boldsymbol{P}_{k|k}$, such that $\boldsymbol{x}_k \in \mathcal{E}(\hat{\boldsymbol{x}}_{k|k}, \boldsymbol{P}_{k|k})$. The corrected state estimate is given by

$$\hat{\boldsymbol{x}}_{k|k} = \hat{\boldsymbol{x}}_{k|k-1} + \boldsymbol{L}_k(\boldsymbol{y}_k - \boldsymbol{C}\hat{\boldsymbol{x}}_{k|k-1}) \tag{2}$$

where $\boldsymbol{L}_k$ is the filter gain. Since $\boldsymbol{x}_k \in \mathcal{E}(\hat{\boldsymbol{x}}_{k|k-1}, \boldsymbol{P}_{k|k-1})$, there exists a $\boldsymbol{z}_{k|k-1} \in \mathbb{R}^{\bar{n}}$ with $|\boldsymbol{z}_{k|k-1}| \leq 1$ such that

$$\boldsymbol{x}_k = \hat{\boldsymbol{x}}_{k|k-1} + \boldsymbol{E}_{k|k-1}\boldsymbol{z}_{k|k-1} \tag{3}$$

where $\boldsymbol{E}_{k|k-1}$ is the Cholesky factorization of $\boldsymbol{P}_{k|k-1}$, i.e., $\boldsymbol{P}_{k|k-1} = \boldsymbol{E}_{k|k-1}\boldsymbol{E}_{k|k-1}^{\mathrm{T}}$ [23,24].

### 2.2 Prediction Step.

At each time-step $k \in \mathbb{Z}_\star$, given $\boldsymbol{x}_k \in \mathcal{E}(\hat{\boldsymbol{x}}_{k|k}, \boldsymbol{P}_{k|k})$ and $\boldsymbol{w}_k \in \mathcal{E}(0_{\bar{w}}, \boldsymbol{Q}_k)$, the objective is to find the optimal prediction ellipsoid, characterized by $\hat{\boldsymbol{x}}_{k+1|k}$ and $\boldsymbol{P}_{k+1|k}$, such that $\boldsymbol{x}_{k+1} \in \mathcal{E}(\hat{\boldsymbol{x}}_{k+1|k}, \boldsymbol{P}_{k+1|k})$ where the predicted state estimate is given by

$$\hat{\boldsymbol{x}}_{k+1|k} = \boldsymbol{A}\hat{\boldsymbol{x}}_{k|k} + \boldsymbol{B}\boldsymbol{u}_k \tag{4}$$

Again, since $\boldsymbol{x}_k \in \mathcal{E}(\hat{\boldsymbol{x}}_{k|k}, \boldsymbol{P}_{k|k})$, we have

$$\boldsymbol{x}_k = \hat{\boldsymbol{x}}_{k|k} + \boldsymbol{E}_{k|k}\boldsymbol{z}_{k|k} \tag{5}$$

where $\boldsymbol{P}_{k|k} = \boldsymbol{E}_{k|k}\boldsymbol{E}_{k|k}^{\mathrm{T}}$ and $|\boldsymbol{z}_{k|k}| \leq 1$. Initialization is provided by $\hat{\boldsymbol{x}}_{0|-1} = \hat{\boldsymbol{x}}_0$ and $\boldsymbol{P}_{0|-1} = \boldsymbol{P}_0$ [19].

*Remark 1.* As mentioned in the filtering objectives, we are interested in finding the optimal ellipsoids, i.e., the minimum-"size" ellipsoids, at each time-step. There are two criteria for the "size" of an ellipsoid in terms of its shape matrix: trace criterion and log-determinant criterion [23]. In this paper, we have considered the trace criterion (see Theorems 1 and 2), which represents the sum of squared lengths of semi-axes of an ellipsoid [23]. As a result, the corresponding optimization problems are convex (see the SDPs in Eqs. (6) and (8)). Alternatively, for minimum-volume ellipsoids, one can consider the log-determinant criterion. However, this would render the optimization problems nonconvex, and additional modifications might be required to restore convexity (see, for example, Ref. [23]).

## 3 Set-Membership Filter Design

In this section, we formulate the SDPs to be solved at each time-step for the SMF. As the SMF design is motivated by the one in Ref. [34], we have adopted the notations and relevant statements provided in Ref. [34]. First, we state the result that summarizes the filtering problem at the correction step.

Theorem 1. *Consider the system in Eq. (1) under the Assumption 1. Then, at each time-step $k \in \mathbb{Z}_\star$, upon receiving the measured output $\boldsymbol{y}_k$ with $\boldsymbol{v}_k \in \mathcal{E}(0_{\bar{v}}, \boldsymbol{R}_k)$ and given $\boldsymbol{x}_k \in \mathcal{E}(\hat{\boldsymbol{x}}_{k|k-1}, \boldsymbol{P}_{k|k-1})$, the state $\boldsymbol{x}_k$ is contained in the optimal* *correction ellipsoid given by* $\mathcal{E}(\hat{\boldsymbol{x}}_{k|k}, \boldsymbol{P}_{k|k})$, *if there exist* $\boldsymbol{P}_{k|k} > 0$, $\boldsymbol{L}_k$, $\tau_i \geq 0$, $i = 1,2$ *as solutions to the following SDP:*

$$\begin{aligned}
&\min_{\boldsymbol{P}_{k|k}, \boldsymbol{L}_k, \tau_1, \tau_2} \ \mathrm{trace}(\boldsymbol{P}_{k|k}) \\
&\text{subject to} \\
&\boldsymbol{P}_{k|k} > 0 \\
&\tau_i \geq 0,\ i = 1,2 \\
&\begin{bmatrix} -\boldsymbol{P}_{k|k} & \boldsymbol{\Pi}_{k|k-1} \\ \boldsymbol{\Pi}_{k|k-1}^{\mathrm{T}} & -\boldsymbol{\Theta}(\tau_1, \tau_2) \end{bmatrix} \leq 0
\end{aligned} \tag{6}$$

*where* $\boldsymbol{\Pi}_{k|k-1}$ *and* $\boldsymbol{\Theta}(\tau_1, \tau_2)$ *are given by*

$$\begin{aligned}
\boldsymbol{\Pi}_{k|k-1} &= [0_{\bar{n}} \quad (\boldsymbol{E}_{k|k-1} - \boldsymbol{L}_k \boldsymbol{C} \boldsymbol{E}_{k|k-1}) \quad -\boldsymbol{L}_k \boldsymbol{D}] \\
\boldsymbol{\Theta}(\tau_1, \tau_2) &= \mathrm{diag}\,(1 - \tau_1 - \tau_2, \tau_1 \boldsymbol{I}_{\bar{n}}, \tau_2 \boldsymbol{R}_k^{-1})
\end{aligned} \tag{7}$$

*Furthermore, the center of the correction ellipsoid is given by the corrected state estimate in Eq. (2).*

*Proof*. Follows from the proof of Theorem 1 in Ref. [34]. ■

Next, we state the technical result for the prediction step.

THEOREM 2. *Consider the system in Eq. (1) under the Assumption 1 with the state* $\boldsymbol{x}_k$ *in the correction ellipsoid* $\mathcal{E}(\hat{\boldsymbol{x}}_{k|k}, \boldsymbol{P}_{k|k})$ *and* $\boldsymbol{w}_k \in \mathcal{E}(0_{\bar{w}}, \boldsymbol{Q}_k)$. *Then, the successor state* $\boldsymbol{x}_{k+1}$ *belongs to the optimal prediction ellipsoid* $\mathcal{E}(\hat{\boldsymbol{x}}_{k+1|k}, \boldsymbol{P}_{k+1|k})$ *if there exist* $\boldsymbol{P}_{k+1|k} > 0$, $\tau_i \geq 0$, $i = 3,4$ *as solutions to the following SDP:*

$$\begin{aligned}
&\min_{\boldsymbol{P}_{k+1|k}, \tau_3, \tau_4} \ \mathrm{trace}(\boldsymbol{P}_{k+1|k}) \\
&\text{subject to} \\
&\boldsymbol{P}_{k+1|k} > 0 \\
&\tau_i \geq 0, i = 3,4 \\
&\begin{bmatrix} -\boldsymbol{P}_{k+1|k} & \boldsymbol{\Pi}_{k|k} \\ \boldsymbol{\Pi}_{k|k}^{\mathrm{T}} & -\boldsymbol{\Psi}(\tau_3, \tau_4) \end{bmatrix} \leq 0
\end{aligned} \tag{8}$$

*where* $\boldsymbol{\Pi}_{k|k}$ *and* $\boldsymbol{\Psi}(\tau_3, \tau_4)$ *are given by*

$$\begin{aligned}
\boldsymbol{\Pi}_{k|k} &= [0_{\bar{n}} \quad \boldsymbol{A}\boldsymbol{E}_{k|k} \quad \boldsymbol{G}] \\
\boldsymbol{\Psi}(\tau_3, \tau_4) &= \mathrm{diag}\,(1 - \tau_3 - \tau_4, \tau_3 \boldsymbol{I}_{\bar{n}}, \tau_4 \boldsymbol{Q}_k^{-1})
\end{aligned}$$

*Furthermore, the center of the prediction ellipsoid is given by the predicted state estimate in Eq. (4).*

*Proof*. Follows from the proof of Theorem 2 in Ref. [34]. ■

Interior point methods can be implemented to efficiently solve the SDPs in Eqs. (6) and (8) [35]. The recursive SMF algorithm is summarized in Algorithm 1.

**Algorithm 1** The SMF Algorithm

1: (Initialization) Select a time-horizon $T_f$. Given the initial values $(\hat{\boldsymbol{x}}_0, \boldsymbol{P}_0)$, set $k=0$, $\hat{\boldsymbol{x}}_{k|k-1} = \hat{\boldsymbol{x}}_0$, $\boldsymbol{E}_{k|k-1} = \boldsymbol{E}_0$ where $\boldsymbol{P}_0 = \boldsymbol{E}_0 \boldsymbol{E}_0^{\mathrm{T}}$.
2: Find $\boldsymbol{P}_{k|k}$ and $\boldsymbol{L}_k$ by solving the SDP in Eq. (6).
3: Calculate $\hat{\boldsymbol{x}}_{k|k}$ using Eq. (2). Also, calculate $\boldsymbol{E}_{k|k}$ using $\boldsymbol{P}_{k|k} = \boldsymbol{E}_{k|k} \boldsymbol{E}_{k|k}^{\mathrm{T}}$.
4: Solve the SDP in Eq. (8) to obtain $\boldsymbol{P}_{k+1|k}$.
5: Calculate $\hat{\boldsymbol{x}}_{k+1|k}$ using Eq. (4). Compute $\boldsymbol{E}_{k+1|k}$ using $\boldsymbol{P}_{k+1|k} = \boldsymbol{E}_{k+1|k} \boldsymbol{E}_{k+1|k}^{\mathrm{T}}$.
6: If $k = T_f$ exit. Otherwise, set $k = k + 1$ and go to Step 2.

## 4 Leader–Follower Synchronization of Multi-Agent Systems

This section describes local control input synthesis for the leader–follower synchronization. Results presented in this section are based on the results given in Ref. [16], and, to be consistent, we have adopted some of the terminologies and notations used in Ref. [16].

**4.1 Graph-Related Preliminaries.** Consider a multi-agent system consisting of $N$ agents [1]. The communication topology of the multi-agent system can be represented by a graph $\mathscr{G} = (\mathscr{V}, \mathscr{E})$, where $\mathscr{V} = \{1, 2, \ldots, N\}$ is a nonempty node set and $\mathscr{E} \subseteq \mathscr{V} \times \mathscr{V}$ is an edge set of ordered pairs of nodes, called edges. Node $i$ in the graph represents agent $i$. We consider simple, directed graphs in this paper. The edge $(i, j)$ in the edge set of a directed graph denotes that node $j$ can obtain information from node $i$, but not necessarily vice versa. If an edge $(i,j) \in \mathscr{E}$, then node $i$ is a neighbor of node $j$. The set of neighbors of node $i$ is denoted as $\mathrm{N}_i$.

The adjacency matrix $\mathscr{A} = [a_{ij}] \in \mathbb{R}^{N \times N}$ of a directed graph $(\mathscr{V}, \mathscr{E})$ is defined such that $a_{ij}$ is a positive weight if $(j,i) \in \mathscr{E}$, and $a_{ij} = 0$ otherwise. The graph Laplacian matrix $\boldsymbol{\mathcal{L}}$ is defined as $\mathscr{L} = \mathscr{D} - \mathscr{A}$, where $\mathscr{D} = [d_{ij}] \in \mathbb{R}^{N \times N}$ is the in-degree matrix with $d_{ij} = 0, i \neq j$ and $d_{ii} = \sum_{j=1}^{N} a_{ij}, i = 1, 2, \ldots, N$. A directed path is a sequence of edges in a directed graph of the form $(i_1, i_2)$, $(i_2, i_3)$, …. The graph $\mathscr{G}$ contains a (directed) spanning tree if there exists a node, called the root node, such that every other node in $\mathscr{V}$ can be connected by a directed path starting from that node.

**4.2 Synchronization: Formulation and Results.** We consider $N$ agents connected via a directed graph and a leader. Agent $i$ $(i = 1, 2, \ldots, N)$ is a dynamical system of the form

$$\begin{aligned}
\boldsymbol{x}_{k+1}^{(i)} &= \boldsymbol{A}\boldsymbol{x}_k^{(i)} + \boldsymbol{B}\boldsymbol{u}_k^{(i)} + \boldsymbol{G}\boldsymbol{w}_k^{(i)} \\
\boldsymbol{y}_k^{(i)} &= \boldsymbol{C}\boldsymbol{x}_k^{(i)} + \boldsymbol{D}\boldsymbol{v}_k^{(i)}, \quad k \in \mathbb{Z}_\star
\end{aligned} \tag{9}$$

where $\boldsymbol{x}_k^{(i)} \in \mathbb{R}^n$, $\boldsymbol{u}_k^{(i)} \in \mathbb{R}^m$, $\boldsymbol{y}_k^{(i)} \in \mathbb{R}^p$, $\boldsymbol{w}_k^{(i)} \in \mathbb{R}^w$, and $\boldsymbol{v}_k^{(i)} \in \mathbb{R}^v$ are the state, control input, measured output, input, and output disturbances for agent $i$, respectively. Clearly, the system described by Eq. (9) is in the form of the system described by Eq. (1). Next, we modify Assumption 1 and impose the following assumptions on the dynamics of agent $i$ $(i = 1, 2, \ldots, N)$.

ASSUMPTION 2.

(2.1) *The initial state* $\boldsymbol{x}_0^{(i)}$ *is unknown. However, it satisfies* $\boldsymbol{x}_0^{(i)} \in \mathcal{E}(\hat{\boldsymbol{x}}_0^{(i)}, \boldsymbol{P}_0^{(i)})$, *where* $\hat{\boldsymbol{x}}_0^{(i)}$ *is a given initial estimate and* $\boldsymbol{P}_0^{(i)}$ *is known. Also,* $|\boldsymbol{P}_0^{(i)}| \leq p_0$ *holds with some* $p_0 > 0$.

(2.2) $\boldsymbol{w}_k^{(i)}$ *and* $\boldsymbol{v}_k^{(i)}$ *are unknown-but-bounded for all* $k \in \mathbb{Z}_\star$. *Also,* $\boldsymbol{w}_k^{(i)} \in \mathcal{E}(0_w, \boldsymbol{Q}_k^{(i)})$ *and* $\boldsymbol{v}_k^{(i)} \in \mathcal{E}(0_v, \boldsymbol{R}_k^{(i)})$ *for all* $k \in \mathbb{Z}_\star$, *where* $\boldsymbol{Q}_k^{(i)}$ and $\boldsymbol{R}_k^{(i)}$ *are known with* $|\boldsymbol{Q}_k^{(i)}| \leq \bar{q}$ *and* $|\boldsymbol{R}_k^{(i)}| \leq \bar{r}$ *for all* $k \in \mathbb{Z}_\star$ *with some* $\bar{q}, \bar{r} > 0$.

Under this assumption, agent $i$ $(i = 1, 2, \ldots, N)$ employs the SMF in Algorithm 1 to estimate its own state. Now, we introduce the following assumption on the system matrices of the agents.

ASSUMPTION 3. $\boldsymbol{B}$ *is full column rank with the pair* $(\boldsymbol{A}, \boldsymbol{B})$ *stabilizable.*

We consider the leader to be a system of the form

$$\boldsymbol{x}_{k+1}^{(0)} = \boldsymbol{A}\boldsymbol{x}_k^{(0)}, \ \boldsymbol{y}_k^{(0)} = \boldsymbol{x}_k^{(0)}, \quad k \in \mathbb{Z}_\star \tag{10}$$

where $\boldsymbol{x}_k^{(0)} \in \mathbb{R}^n$ are the leader's state and $\boldsymbol{y}_k^{(0)}$ is the output. Note that the leader is a virtual system that generates the reference trajectory for the agents $i = 1, 2, \ldots, N$ to track. We define the local neighborhood tracking errors, using the corrected state estimates of the agents, as

$$\epsilon_k^{(i)} = \sum_{j \in \mathrm{N}_i} a_{ij} (\hat{\boldsymbol{x}}_{k|k}^{(j)} - \hat{\boldsymbol{x}}_{k|k}^{(i)}) + g_i (\boldsymbol{x}_k^{(0)} - \hat{\boldsymbol{x}}_{k|k}^{(i)})$$

where $g_i \geq 0$ are the pinning gains, $\hat{\boldsymbol{x}}_{k|k}^{(i)}$ and $\hat{\boldsymbol{x}}_{k|k}^{(j)}$ are the corrected state estimates of agent $i$ and $j$, respectively. If agent $i$ is pinned to the leader, we take $g_i > 0$. Now, we choose the control input of agent $i$ as [16]

$$u_k^{(i)} = c(1 + d_{ii} + g_i)^{-1} \boldsymbol{K}\epsilon_k^{(i)}$$

where $c > 0$ is a coupling gain and $\boldsymbol{K}$ is a control gain matrix to be discussed subsequently. Hence, the global dynamics of the $N$ agents can be expressed as

$$\boldsymbol{x}_{k+1}^{(g)} = (\boldsymbol{I}_N \otimes \boldsymbol{A})\boldsymbol{x}_k^{(g)} + \boldsymbol{u}_k^{(g)} + (\boldsymbol{I}_N \otimes \boldsymbol{G})\boldsymbol{w}_k^{(g)}, \quad k \in \mathbb{Z}_\star \tag{11}$$

with $\boldsymbol{x}_k^{(g)} = \text{col}[\boldsymbol{x}_k^{(1)}, \ldots, \boldsymbol{x}_k^{(N)}]$, $\boldsymbol{w}_k^{(g)} = \text{col}[\boldsymbol{w}_k^{(1)}, \ldots, \boldsymbol{w}_k^{(N)}]$, and

$$\begin{aligned} \boldsymbol{u}_k^{(g)} =& -c(\boldsymbol{I}_N + \mathcal{D} + \mathcal{G})^{-1}(\mathcal{L} + \mathcal{G}) \otimes \boldsymbol{BK}\hat{\boldsymbol{x}}_{k|k}^{(g)} \\ &+ c(\boldsymbol{I}_N + \mathcal{D} + \mathcal{G})^{-1}(\mathcal{L} + \mathcal{G}) \otimes \boldsymbol{BK}\bar{\boldsymbol{x}}_k^{(0)} \end{aligned} \tag{12}$$

where $\mathcal{G} = \text{diag}(g_1, g_2, \ldots, g_N)$ is the matrix of pinning gains, $\hat{\boldsymbol{x}}_{k|k}^{(g)} = \text{col}[\hat{\boldsymbol{x}}_{k|k}^{(1)}, \ldots, \hat{\boldsymbol{x}}_{k|k}^{(N)}]$, and $\bar{\boldsymbol{x}}_k^{(0)} = (1_N \otimes \boldsymbol{x}_k^{(0)})$. Note that the superscript $(g)$ is utilized to denote the global variables. Now, using Eq. (5) for each agent's corrected state estimates, we can express $\boldsymbol{x}_k^{(g)}$ as

$$\boldsymbol{x}_k^{(g)} = \hat{\boldsymbol{x}}_{k|k}^{(g)} + \boldsymbol{E}_{k|k}^{(g)}\boldsymbol{z}_{k|k}^{(g)} \tag{13}$$

where $\boldsymbol{E}_{k|k}^{(g)} = \text{diag}(\boldsymbol{E}_{k|k}^{(1)}, \ldots, \boldsymbol{E}_{k|k}^{(N)})$, $\boldsymbol{z}_{k|k}^{(g)} = \text{col}[\boldsymbol{z}_{k|k}^{(1)}, \ldots, \boldsymbol{z}_{k|k}^{(N)}]$. Note that $\boldsymbol{E}_{k|k}^{(i)}(\boldsymbol{E}_{k|k}^{(i)})^{\text{T}} = \boldsymbol{P}_{k|k}^{(i)}$, where $\boldsymbol{P}_{k|k}^{(i)}$ is the correction ellipsoid shape matrix for agent $i$ and $|\boldsymbol{z}_{k|k}^{(i)}| \leq 1$ for $i = 1, \ldots, N$. Our next assumption is regarding the interaction graph.

Assumption 4 [16]. *The interaction graph contains a spanning tree with at least one nonzero pinning gain that connects the leader and the root node.*

The global disagreement error [16] is defined as $\boldsymbol{\delta}_k^{(g)} = \boldsymbol{x}_k^{(g)} - \bar{\boldsymbol{x}}_k^{(0)}$. Utilizing Eqs. (11)–(13), we express the global error system as

$$\boldsymbol{\delta}_{k+1}^{(g)} = \boldsymbol{A}_c\boldsymbol{\delta}_k^{(g)} + \boldsymbol{B}_c\boldsymbol{E}_{k|k}^{(g)}\boldsymbol{z}_{k|k}^{(g)} + (\boldsymbol{I}_N \otimes \boldsymbol{G})\boldsymbol{w}_k^{(g)}, \quad k \in \mathbb{Z}_\star \tag{14}$$

where

$$\boldsymbol{A}_c = [(\boldsymbol{I}_N \otimes \boldsymbol{A}) - c\boldsymbol{\Gamma} \otimes \boldsymbol{BK}], \; \boldsymbol{B}_c = c\boldsymbol{\Gamma} \otimes \boldsymbol{BK} \tag{15}$$

with $\boldsymbol{\Gamma} = (\boldsymbol{I}_N + \mathcal{D} + \mathcal{G})^{-1}(\mathcal{L} + \mathcal{G})$. Now, we recall the following technical result from Ref. [16].

Lemma 1 [16]. $\rho(\boldsymbol{A}_c) < 1$ *iff* $\rho(\boldsymbol{A} - c\Lambda_i\boldsymbol{BK}) < 1$ *for all the eigenvalues* $\Lambda_i, i = 1, 2, \ldots, N$ *of* $\boldsymbol{\Gamma}$.

If the matrix $\boldsymbol{A}$ is unstable or marginally stable, then Lemma 1 requires Assumption 4 with the pair $(\boldsymbol{A}, \boldsymbol{B})$ stabilizable [16]. Using Theorem 2 in Ref. [16], $c$ and $\boldsymbol{K}$ are chosen such that $\rho(\boldsymbol{A}_c) < 1$. To this end, we state the following result.

Lemma 2 [16]. *Let Assumption 4 holds, and let* $\mathcal{P}$ *be a positive definite solution to the discrete-time Riccati-like equation*

$$\boldsymbol{A}^{\text{T}}\mathcal{P}\boldsymbol{A} - \mathcal{P} + \mathcal{Q} - \boldsymbol{A}^{\text{T}}\mathcal{P}\boldsymbol{B}(\boldsymbol{B}^{\text{T}}\mathcal{P}\boldsymbol{B})^{-1}\boldsymbol{B}^{\text{T}}\mathcal{P}\boldsymbol{A} = \boldsymbol{O}_n \tag{16}$$

*for some* $\mathcal{Q} > 0$. *Define*

$$r = [\sigma_{\max}(\mathcal{Q}^{-0.5}\boldsymbol{A}^{\text{T}}\mathcal{P}\boldsymbol{B}(\boldsymbol{B}^{\text{T}}\mathcal{P}\boldsymbol{B})^{-1}\boldsymbol{B}^{\text{T}}\mathcal{P}\boldsymbol{A}\,\mathcal{Q}^{-0.5})]^{-0.5}$$

Furthermore, let there exists a $C(c_0, r_0)$ containing all the eigenvalues $\Lambda_i, i = 1, 2, \ldots, N$ of $\boldsymbol{\Gamma}$ such that $(r_0/c_0) < r$. Then, $\rho(\boldsymbol{A}_c) < 1$ for $\boldsymbol{K} = (\boldsymbol{B}^{\text{T}}\mathcal{P}\boldsymbol{B})^{-1}\boldsymbol{B}^{\text{T}}\mathcal{P}\boldsymbol{A}$ and $c = (1/c_0)$.

If $\boldsymbol{B}$ is a full column rank, Eq. (16) has a positive definite solution $\mathcal{P}$ only if the pair $(\boldsymbol{A}, \boldsymbol{B})$ is stabilizable [16]. In this regard, Assumption 3 is pertinent. Next, we introduce the notion of input-to-state stability in the following definition.

Definition 2. *A discrete-time system of the form* $\boldsymbol{x}_{k+1} = \phi(\boldsymbol{x}_k, \boldsymbol{u}_{1_k}, \boldsymbol{u}_{2_k})$, $k \in \mathbb{Z}_\star$ *with* $\boldsymbol{u}_1 : \mathbb{Z}_\star \to \mathbb{R}^{m_1}$, $\boldsymbol{u}_2 : \mathbb{Z}_\star \to \mathbb{R}^{m_2}$, $\phi(0_n, 0_{m_1}, 0_{m_2}) = 0_n$ *is (globally) ISS if there exist a class* $\mathcal{KL}$ *function* $\beta$ *and two class* $\mathcal{K}$ *functions* $\gamma_1, \gamma_2$ *such that, for each pair of inputs* $\boldsymbol{u}_1 \in l_\infty^{m_1}$, $\boldsymbol{u}_2 \in l_\infty^{m_2}$ *and each* $\boldsymbol{x}_0 \in \mathbb{R}^n$, *it holds that*

$$|\boldsymbol{x}_k| \leq \beta(|\boldsymbol{x}_0|, k) + \gamma_1(||\boldsymbol{u}_1||) + \gamma_2(||\boldsymbol{u}_2||) \tag{17}$$

*for each* $k \in \mathbb{Z}_\star$.

*Remark* 2. Definition 2 is adopted from Definition 3.1 in Ref. [32] and has been suitably modified for systems with two inputs using Definition IV.3 in Ref. [33].

We state the main result of this section in Theorem 3.

Theorem 3. *Suppose the following conditions are satisfied: (i) Under Assumption 2, agent i (i = 1, 2, ..., N) employs the SMF in Algorithm 1 to estimate its own state; (ii) Assumptions 3 and 4 hold; (iii) c and* $\boldsymbol{K}$ *are chosen using Lemma 2. Then, the global error system in Eq. (14) is ISS.*

*Proof.* The proof is inspired by Example 3.4 in Ref. [32]. Let us denote $\boldsymbol{e}_k^{(g)} = \text{col}[\boldsymbol{e}_k^{(1)}, \ldots, \boldsymbol{e}_k^{(N)}]$, where $\boldsymbol{e}_k^{(i)} = \boldsymbol{x}_k^{(i)} - \hat{\boldsymbol{x}}_{k|k}^{(i)}$ is the state estimation errors of agent $i$ at the correction steps. Now, using Eq. (13), we have $\boldsymbol{e}_k^{(g)} = \boldsymbol{x}_k^{(g)} - \hat{\boldsymbol{x}}_{k|k}^{(g)} = \boldsymbol{E}_{k|k}^{(g)}\boldsymbol{z}_{k|k}^{(g)}$. Similarly, let us denote $\boldsymbol{e}_0^{(g)} = \text{col}[\boldsymbol{e}_0^{(1)}, \ldots, \boldsymbol{e}_0^{(N)}]$, where $\boldsymbol{e}_0^{(i)} = \boldsymbol{x}_0^{(i)} - \hat{\boldsymbol{x}}_0^{(i)}$ is the initial estimation error of agent $i$. Due to Assumption 2, we have

$$\boldsymbol{e}_0^{(g)} = \boldsymbol{E}_0^{(g)}\boldsymbol{z}_0^{(g)} \tag{18}$$

with $\boldsymbol{E}_0^{(g)} = \text{diag}(\boldsymbol{E}_0^{(1)}, \ldots, \boldsymbol{E}_0^{(N)})$, $\boldsymbol{z}_0^{(g)} = \text{col}[\boldsymbol{z}_0^{(1)}, \ldots, \boldsymbol{z}_0^{(N)}]$, where $\boldsymbol{E}_0^{(i)}(\boldsymbol{E}_0^{(i)})^{\text{T}} = \boldsymbol{P}_0^{(i)}$ and $|\boldsymbol{z}_0^{(i)}| \leq 1$ for $i = 1, \ldots, N$. Then, Eq. (14) becomes

$$\boldsymbol{\delta}_{k+1}^{(g)} = \boldsymbol{A}_c^{k+1}\boldsymbol{\delta}_0^{(g)} + \sum_{j=0}^{k}\boldsymbol{A}_c^j\boldsymbol{B}_c\boldsymbol{e}_{k-j}^{(g)} + \sum_{j=0}^{k}\boldsymbol{A}_c^j(\boldsymbol{I}_N \otimes \boldsymbol{G})\boldsymbol{w}_{k-j}^{(g)}$$

where $\boldsymbol{e}^{(g)} : \mathbb{Z}_\star \to \mathbb{R}^{nN}$ and $\boldsymbol{w}^{(g)} : \mathbb{Z}_\star \to \mathbb{R}^{wN}$ are the inputs. It is understood that $\boldsymbol{e}^{(g)} \in l_\infty^{nN}$ and $\boldsymbol{w}^{(g)} \in l_\infty^{wN}$. Due to the choices of $c$ and $\boldsymbol{K}$ along with Assumptions 3 and 4, we have $\rho(\boldsymbol{A}_c) < 1$. Hence, there exist constants $\alpha > 0$ and $\mu \in [0, 1)$, such that $|\boldsymbol{A}_c^k| \leq \alpha\mu^k$, $k \in \mathbb{Z}_\star$ [32]. Then, the ISS property in Eq. (17) holds for the system in Eq. (14) with

$$\begin{aligned} \beta(s, k) = \alpha\mu^k s, \; \gamma_1(s_1) &= \sum_{j=0}^{\infty}\alpha\mu^j|\boldsymbol{B}_c|s_1 = \frac{\alpha|\boldsymbol{B}_c|s_1}{1 - \mu} \\ \gamma_2(s_2) &= \sum_{j=0}^{\infty}\alpha\mu^j|\boldsymbol{G}|s_2 = \frac{\alpha|\boldsymbol{G}|s_2}{1 - \mu} \end{aligned} \tag{19}$$

where $|(\boldsymbol{I}_N \otimes \boldsymbol{G})| = |\boldsymbol{I}_N|\,|\boldsymbol{G}| = |\boldsymbol{G}|$ is utilized. Thus, along the trajectories of the system in Eq. (14), for each $k \in \mathbb{Z}_\star$, it holds that

$$|\boldsymbol{\delta}_k^{(g)}| \leq \beta(|\boldsymbol{\delta}_0^{(g)}|, k) + \gamma_1(||\boldsymbol{e}^{(g)}||) + \gamma_2(||\boldsymbol{w}^{(g)}||) \tag{20}$$

where the functions $\beta, \gamma_1$, and $\gamma_2$ are as in Eq. (19) with $s = |\boldsymbol{\delta}_0^{(g)}|$, $s_1 = ||\boldsymbol{e}^{(g)}||$, and $s_2 = ||\boldsymbol{w}^{(g)}||$. ■

Theorem 3 implies that the global disagreement error remains bounded under the proposed synchronization protocol.

*Remark* 3. Objective of the SMF-based synchronization in Ref. [31] was to contain the states of the agents in a confidence ellipsoid that might not be small in general. Thus, the approach outlined in Ref. [31] may lead to conservative results where the states of the agents might not converge to a neighborhood of the leader's state trajectory. On the other hand, we have shown that, under appropriate conditions, the global error system is ISS with respect to the input disturbances and estimation errors. Since an ISS system admits the "converging-input converging-state" property (see, Refs. [32] and [36] for details), $|\boldsymbol{\delta}_k^{(g)}|$ would eventually converge to a neighborhood of zero as the estimation errors of the agents decrease. Thus, the agents would converge to a neighborhood of the leader's state trajectory. To this end, it is understood that $||\boldsymbol{w}^{(g)}||$ is relatively small (compared to $|\boldsymbol{\delta}_0^{(g)}|$ and $||\boldsymbol{e}^{(g)}||$) as the input disturbances satisfy Assumption 2.2.

Next, we state the following result based on Theorem 3, where $p_0$ and $\bar{q}$ are as in Assumption 2.

COROLLARY 1. *Under the conditions of Theorem 3, the normalized global disagreement error* $\bar{\boldsymbol{\delta}}_k^{(g)}$ *satisfies*

$$\lim_{k\to\infty} |\bar{\boldsymbol{\delta}}_k^{(g)}| \le (|\boldsymbol{B}_c|\sqrt{p_0} + |\boldsymbol{G}|\sqrt{\bar{q}}) \tag{21}$$

*with* $\bar{\boldsymbol{\delta}}_k^{(g)} = (\boldsymbol{\delta}_k^{(g)}/\bar{\mu})$, *where* $\bar{\mu} = (\alpha\sqrt{N}/(1-\mu))$ *and* $\alpha > 0$, $\mu \in [0,1)$ *are such that* $|\boldsymbol{A}_c^k| \le \alpha\mu^k$ *for all* $k \in \mathbb{Z}_\star$.

*Proof*. Under the conditions of Theorem 3, the result in Eq. (20) holds. Then, let us rewrite Eq. (20) as

$$|\boldsymbol{\delta}_k^{(g)}| \le \alpha\mu^k|\boldsymbol{\delta}_0^{(g)}| + (\alpha/(1-\mu))(|\boldsymbol{B}_c|\,||\boldsymbol{e}^{(g)}|| + |\boldsymbol{G}|\,||\boldsymbol{w}^{(g)}||)$$

Now, under the assumption that the SMFs of the agents are performing adequately, we can utilize Eq. (18) and take $||\boldsymbol{e}^{(g)}|| \le |\boldsymbol{e}_0^{(g)}| \le |\boldsymbol{E}_0^{(g)}|\,|\boldsymbol{z}_0^{(g)}|$. Using Assumption 2, we have $|\boldsymbol{E}_0^{(g)}| = \max(|\boldsymbol{E}_0^{(1)}|, \ldots, |\boldsymbol{E}_0^{(N)}|) \Rightarrow |\boldsymbol{E}_0^{(g)}| \le \sqrt{p_0}$. Also, we have $|\boldsymbol{z}_0^{(g)}| \le \sqrt{N}$. Therefore, we derive $||\boldsymbol{e}^{(g)}|| \le \sqrt{p_0 N}$. Similarly, Assumption 2 leads to $||\boldsymbol{w}^{(g)}|| \le \sqrt{\bar{q}N}$. Combining these, we calculate the following bound on $\boldsymbol{\delta}_k^{(g)}$

$$|\boldsymbol{\delta}_k^{(g)}| \le \alpha\mu^k|\boldsymbol{\delta}_0^{(g)}| + \bar{\mu}(|\boldsymbol{B}_c|\sqrt{p_0} + |\boldsymbol{G}|\sqrt{\bar{q}}) \tag{22}$$

for each $k \in \mathbb{Z}_\star$ with $\bar{\mu} = (\alpha\sqrt{N}/(1-\mu))$. Hence, the proof is completed by taking the limit in Eq. (21) and carrying out the normalization $\bar{\boldsymbol{\delta}}_k^{(g)} = (\boldsymbol{\delta}_k^{(g)}/\bar{\mu})$. ■

*Remark 4*. The upper bound shown in Eq. (22) is monotonically decreasing. The estimate given in Eq. (21) is a conservative one as we have utilized $||\boldsymbol{e}^{(g)}|| \le \sqrt{p_0 N}$ and $||\boldsymbol{w}^{(g)}|| \le \sqrt{\bar{q}N}$. Also, the bound $|\boldsymbol{R}_k^{(i)}| \le \bar{r}$ does not appear in Eqs. (21) and (22) as a result of utilizing $||\boldsymbol{e}^{(g)}|| \le |\boldsymbol{e}_0^{(g)}| \le |\boldsymbol{E}_0^{(g)}|\,|\boldsymbol{z}_0^{(g)}|$. However, the true value of $\boldsymbol{e}_k^{(i)}$ would depend on $\boldsymbol{v}_k^{(i)}$ and, thus, on $\boldsymbol{R}_k^{(i)}$ for all $k \in \mathbb{Z}_\star$ and all $i = 1, 2, \ldots, N$.

*Remark 5*. For a given multi-agent system (with the number of agents $N$, the matrices $\boldsymbol{A}$, $\boldsymbol{B}$, $\boldsymbol{C}$, $\boldsymbol{D}$, and $\boldsymbol{G}$, and the interaction graph specified), we have $|\boldsymbol{B}_c|$ and $|\boldsymbol{G}|$ fixed once $c$ and $\boldsymbol{K}$ are properly chosen using Lemma 2. Thus, the conservatism of the bound in Eq. (21) can be reduced if the available upper bounds (i.e., $p_0$ and $\bar{q}$) are sufficiently small.

## 5 Simulation Example

A simulation example is provided in this section to illustrate the effectiveness of the proposed SMF-based leader–follower synchronization protocol. All the simulations are carried out on a desktop computer with a 16.00 GB RAM and a 3.40 GHz Intel(R) Xeon(R) E-2124 G processor running MATLAB R2019a. The SDPs in Eqs. (6) and (8) are solved utilizing "YALMIP" [37] with the "SDPT3" solver in the MATLAB framework. Since the disturbances are only assumed to be unknown-but-bounded, different kinds of disturbance realizations are possible, which satisfy the ellipsoidal assumptions (Assumptions 1.2 and 2.2), for example, periodic disturbances with time-varying or constant frequencies and amplitudes, random disturbances with each element being uniformly distributed in an interval, and so on.

We consider four agents, i.e., $N = 4$. Matrices related to the dynamics of the leader and the agents are

$$\boldsymbol{A} = \begin{bmatrix} 0 & -1 \\ 1 & 0 \end{bmatrix}, \boldsymbol{B} = \boldsymbol{I}_2, \boldsymbol{C} = [1 \quad 0], \boldsymbol{D} = 1, \boldsymbol{G} = \boldsymbol{I}_2 \tag{23}$$

where $\boldsymbol{A}$ is marginally stable. Also, Assumption 3 is satisfied with the above choices of $\boldsymbol{A}$ and $\boldsymbol{B}$. Ellipsoidal parameters related to

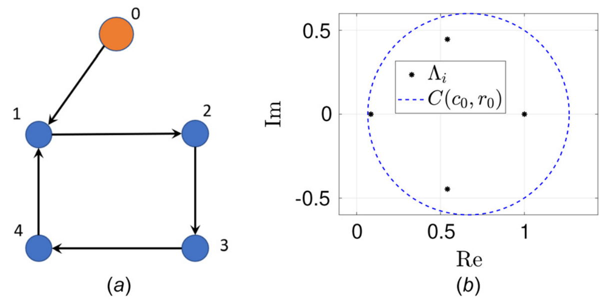


**Fig. 1 (*a*) The interaction graph and (*b*) eigenvalues of $\Gamma$ ($\Lambda_i$, $i = 1, 2, 3,$ and 4) in the complex plane with $C(c_0, r_0)$**

the SMFs of the agents are $\boldsymbol{P}_0^{(i)} = 2\boldsymbol{I}_2$, $\boldsymbol{Q}_k^{(i)} = 0.1\boldsymbol{I}_2$, and $\boldsymbol{R}_k^{(i)} = 0.1$ for $i = 1, 2, 3,$ and 4. The initial state estimates of the agents are as follows: $\hat{\boldsymbol{x}}_0^{(1)} = [50 \quad -50]^{\mathrm{T}}$, $\hat{\boldsymbol{x}}_0^{(2)} = \hat{\boldsymbol{x}}_0^{(1)}$, $\hat{\boldsymbol{x}}_0^{(3)} = [-50 \quad 50]^{\mathrm{T}}$, and $\hat{\boldsymbol{x}}_0^{(4)} = \hat{\boldsymbol{x}}_0^{(3)}$. The true initial state for the agents 1 and 2 ($\boldsymbol{x}_0^{(1)}$, $\boldsymbol{x}_0^{(2)}$) are chosen randomly (uniform distribution) between $[50 \quad -50]^{\mathrm{T}}$ and $[51 \quad -49]^{\mathrm{T}}$. Similarly, the true initial state for the agents 3 and 4 ($\boldsymbol{x}_0^{(3)}$, $\boldsymbol{x}_0^{(4)}$) is chosen randomly (uniform distribution) between $[-50 \quad 50]^{\mathrm{T}}$ and $[-49 \quad 51]^{\mathrm{T}}$. The input

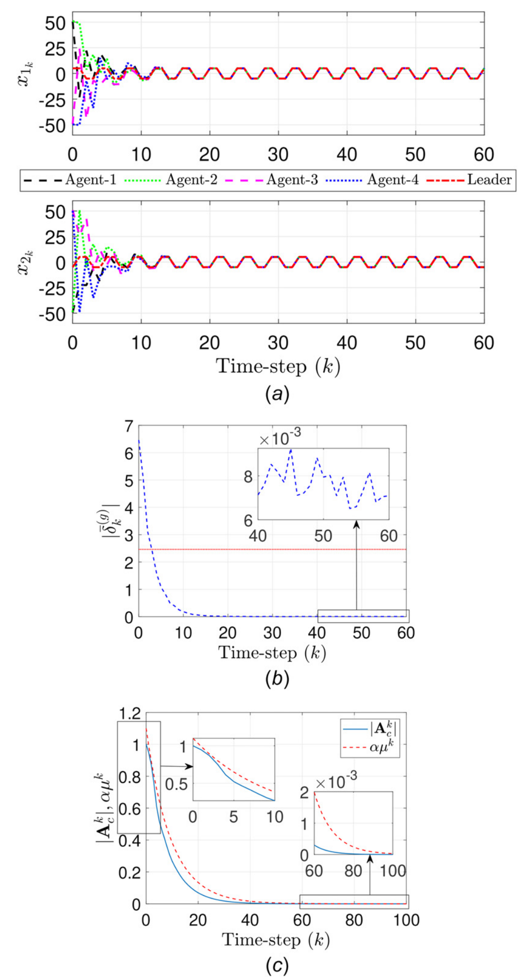


**Fig. 2 Simulation results for the example: (*a*) true states of the leader and the agents, (*b*) normalized global disagreement error norm, and (*c*) $|\boldsymbol{A}_c^k|$ and the upper bound**

disturbances ($\boldsymbol{w}_k^{(i)}$, $i = 1,2,3,4$) are chosen randomly (uniform distribution) between $-0.05\mathbf{1}_2$ and $0.05\mathbf{1}_2$, and the output disturbances ($\boldsymbol{v}_k^{(i)}$, $i = 1,2,3,4$) are chosen randomly (uniform distribution) between $-0.05$ and $0.05$. Thus, Assumption 2 has been satisfied with the above parameters, initial conditions, and disturbance terms. The initial state of the leader is chosen as $\boldsymbol{x}_0^{(0)} = [5 \; -5]^{\mathrm{T}}$.

The interaction graph is shown in Fig. 1(*a*), and Assumption 4 holds for this interaction graph. Thus, we have

$$\mathcal{L} = \begin{bmatrix} 1 & 0 & 0 & -1 \\ -1 & 1 & 0 & 0 \\ 0 & -1 & 1 & 0 \\ 0 & 0 & -1 & 1 \end{bmatrix} \tag{24}$$

$\mathcal{G} = \mathrm{diag}(1,0,0,0)$, $\mathcal{D} = \mathrm{diag}(1,1,1,1)$. With regards to Lemma 2, we choose $\mathcal{Q} = 0.1\boldsymbol{I}_2$, $c_0 = (2/3)$, $r_0 = 0.6$. Clearly, $C(c_0, r_0)$ contains all the eigenvalues of $\boldsymbol{\Gamma}$, as shown in Fig. 1(*b*). Also, we have $r = 1$ and $(r_0/c_0) = 0.9 < r$. Hence, the conditions for Lemma 2 are satisfied, and we take $c = (1/c_0) = 1.5$, $\boldsymbol{K} = (\boldsymbol{B}^{\mathrm{T}}\mathcal{P}\boldsymbol{B})^{-1}\boldsymbol{B}^{\mathrm{T}}\mathcal{P}\boldsymbol{A}$.

The synchronization results are shown in Figs. 2(*a*) and 2(*b*). Figure 2(*a*) shows that the trajectories of the agents converge close to that of the leader. As a result, the normalized global disagreement error norm converges to a neighborhood of zero (Fig. 2(*b*)). The dotted line in Fig. 2(*b*) denotes the conservative bound in Eq. (21) for which we have utilized $p_0 = 2$ and $\bar{q} = 0.1$. Also, for $\bar{\mu}$, we have taken $\alpha = 1.1$ and $\mu = 0.9$. For this choice of $\alpha$ and $\mu$, $|\boldsymbol{A}_c^k| \le \alpha\mu^k$ is satisfied, as shown in Fig. 2(*c*). With the above values, the conservative upper bound is equal to 2.462, which is shown using the dotted line in Fig. 2(*b*).

The estimation results corresponding to the SMFs of the agents are shown in Figs. 3–6. The estimation errors (at the correction steps) for agent $i$'s SMF are denoted by $\boldsymbol{e}_k^{(i)} = [e_{1_k}^{(i)} \quad e_{2_k}^{(i)}]^{\mathrm{T}}$, and the initial errors are denoted by $\boldsymbol{e}_0^{(i)} = \boldsymbol{x}_0^{(i)} - \hat{\boldsymbol{x}}_0^{(i)}$ $(i = 1,2,3,4)$. Figures 3 and 4 show that the SMFs for the agents perform adequately as the estimation errors remain in a neighborhood of zero and the error bounds decrease from the respective initial values. Also, the estimation errors are contained within the error bounds, which mean the SMFs of the agents are able to contain the respective true states inside the respective correction ellipsoids. The estimation error norms, shown in Fig. 5, further illustrate the effectiveness of the SMFs and demonstrate that the SMFs are able to reduce the estimation errors from the respective initial values, starting from the correction step at $k = 0$. The results in Fig. 5 essentially verify our earlier use of $||\boldsymbol{e}^{(g)}|| \le |\boldsymbol{e}_0^{(g)}|$ in deriving the conservative bound in Eq. (21). The trace of correction ellipsoid shape matrices for the SMFs of the agents is shown in Fig. 6, where $\boldsymbol{P}_{k|k}^{(i)}$ $(i = 1,2,3,4)$ denote the shape matrices of agent $i$'s correction ellipsoids. Clearly, SMFs of the agents are able to reduce the trace from the initial values and construct optimal (minimum trace) correction ellipsoids at each time-step (starting from $k = 0$). Quantitatively, the trace of these shape matrices converges approximately to 1.5 (see Fig. 6), which is approximately a 2.667-fold decrease with respect to the initial trace of 4. The trends shown in Fig. 6 for all the agents are roughly the same, as the same set of ellipsoidal parameters is utilized for the SMFs of all the agents and the agents have identical dynamics.

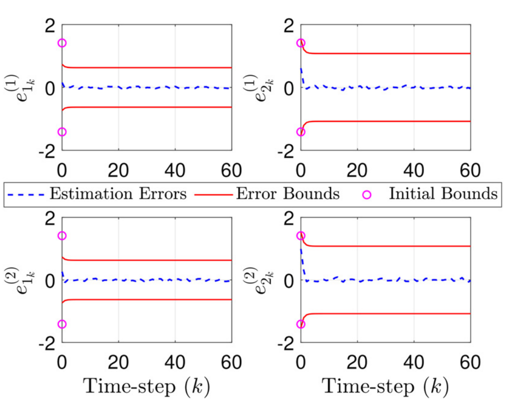


**Fig. 3 Estimation results for SMFs of agents 1 and 2**

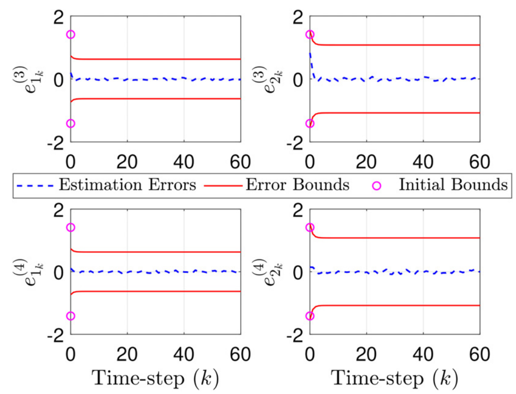


**Fig. 4 Estimation results for SMFs of agents 3 and 4**

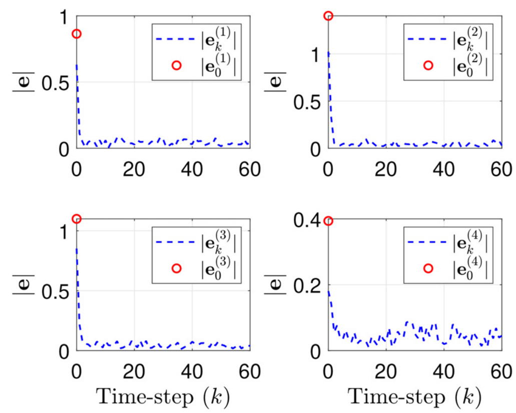


**Fig. 5 Estimation error norms for SMFs of the agents**

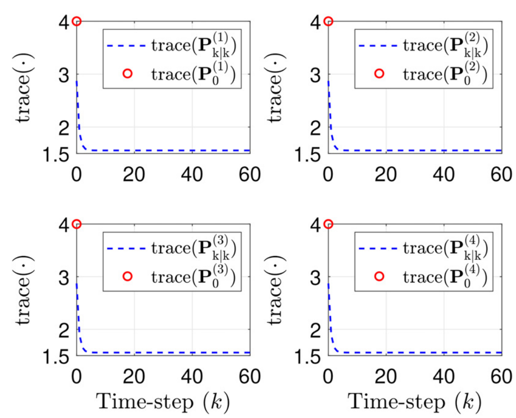


**Fig. 6 Trace of correction ellipsoid shape matrices for SMFs of the agents**

**Table 1** $|\bar{\delta}_k|$ **comparisons over** $T = 61$ **time-steps (**$T_f = 60$**)**

| Disturbance parameters | $\frac{1}{T}\sum_{k=0}^{T_f} \lvert\bar{\delta}_k\rvert$ | $\sqrt{\frac{1}{T}\sum_{k=0}^{T_f} \lvert\bar{\delta}_k\rvert^2}$ |
|---|---|---|
| $\alpha_w = \alpha_v = 0.05$, $Q_k^{(i)} = 0.1I_2$, $R_k^{(i)} = 0.1$ | 0.3706 | 1.1985 |
| $\alpha_w = \alpha_v = 0.5$, $Q_k^{(i)} = I_2$, $R_k^{(i)} = 1$ | 0.4219 | 1.2052 |
| $\alpha_w = \alpha_v = 1$, $Q_k^{(i)} = 2I_2$, $R_k^{(i)} = 1$ | 0.4730 | 1.2124 |

Finally, consider this example with different values of $w_k^{(i)}$, $v_k^{(i)}$, $Q_k^{(i)}$, and $R_k^{(i)}$ $(i = 1, 2, 3,$ and $4)$ while keeping all other conditions and parameters unchanged. Now, let us allow for higher magnitudes of disturbances (with $Q_k^{(i)}$, $R_k^{(i)}$ properly chosen such that Assumption 2 is satisfied) and compare $|\bar{\delta}_k|$ results with the one given in Fig. 2(*b*). Results of this study are given in Table 1 where the following two comparison metrics are used: (i) $\frac{1}{T}\sum_{k=0}^{T_f} |\bar{\delta}_k|$: mean value of $|\bar{\delta}_k|$; (ii) $\sqrt{\frac{1}{T}\sum_{k=0}^{T_f} |\bar{\delta}_k|^2}$: root-mean-square value of $|\bar{\delta}_k|$. Also, $w_k^{(i)}$ is chosen randomly (uniform distribution) between $-\alpha_w 1_2$ and $\alpha_w 1_2$, and $v_k^{(i)}$ is chosen randomly (uniform distribution) between $-\alpha_v$ and $\alpha_v$. Thus, the first row in Table 1 corresponds to the result in Fig. 2(*b*). We observe that both the metrics in Table 1 are comparable among the three cases studied, despite the higher magnitudes of disturbances considered for the two cases in second and third rows of Table 1. Therefore, the $|\bar{\delta}_k|$ trends for these two cases with higher disturbance magnitudes would be qualitatively similar to the one shown in Fig. 2(*b*).

## 6 Conclusion

A set-membership filtering-based leader–follower synchronization protocol for high-order discrete-time linear multi-agent systems has been put forward for which the global error system is shown to be input-to-state stable with respect to the input disturbances and estimation errors. A monotonically decreasing upper bound on the norm of the global disagreement error vector is calculated. Our future work would involve extending the proposed formulation for discrete-time nonlinear dynamical systems and switching network topologies. Also, we would extend the results in this paper by considering a control input for the leader or the leader to be any bounded reference trajectory.


## Funding Data

- Office of Naval Research (Grant No. N00014-18-1-2215; Funder ID: 10.13039/100000006).
- National Science Foundation ("S&AS:FND: Safe Task-Aware Autonomous Resilient Systems (STAARS)," Award No. 1724248; Funder ID: 10.13039/100000001).


## References


[1] Ren, W., and Beard, R. W., 2008, *Distributed Consensus in Multi-Vehicle Cooperative Control*, Springer, London.

[2] Fax, J. A., and Murray, R. M., 2004, "Information Flow and Cooperative Control of Vehicle Formations," IEEE Trans. Autom. Control, **49**(9), pp. 1465–1476.

[3] Murray, R. M., 2007, "Recent Research in Cooperative Control of Multivehicle Systems," ASME J. Dyn. Syst. Meas. Control, **129**(5), pp. 571–583.

[4] Li, Z., Duan, Z., Chen, G., and Huang, L., 2009, "Consensus of Multiagent Systems and Synchronization ofComplex Networks: A Unified Viewpoint," IEEE Trans. Circuits Syst. I, **57**(1), pp. 213–224.

[5] Wu, J., Ugrinovskii, V., and Allgöwer, F., 2014, "Cooperative Estimation for Synchronization of Heterogeneous Multi-Agent Systems Using Relative Information," IFAC Proc. Vol., **47**(3), pp. 4662–4667.

[6] Bhusal, R., and Subbarao, K., 2019, "Sensitivity Analysis of Cooperating Multi-Agent Systems With Uncertain Connection Weights," American Control Conference (ACC), Philadelphia, PA, July 10–12, pp. 4024–4029.

[7] Trentelman, H. L., Takaba, K., and Monshizadeh, N., 2013, "Robust Synchronization of Uncertain Linear Multi-Agent Systems," IEEE Trans. Autom. Control, **58**(6), pp. 1511–1523.

[8] Wang, X., Zhu, J., and Cheng, Z., 2015, "Synchronization Reachable Topology and Synchronization of Discrete-Time Linear Multi-Agent Systems," IEEE Trans. Autom. Control, **60**(7), pp. 1927–1932.

[9] Back, J., and Kim, J.-S., 2017, "Output Feedback Practical Coordinated Tracking of Uncertain Heterogeneous Multi-Agent Systems Under Switching Network Topology," IEEE Trans. Autom. Control, **62**(12), pp. 6399–6406.

[10] Li, Z., Wen, G., Duan, Z., and Ren, W., 2015, "Designing Fully Distributed Consensus Protocols for Linear Multi-Agent Systems With Directed Graphs," IEEE Trans. Autom. Control, **60**(4), pp. 1152–1157.

[11] Lewis, F. L., Cui, B., Ma, T., Song, Y., and Zhao, C., 2016, "Heterogeneous Multi-Agent Systems: Reduced-Order Synchronization and Geometry," IEEE Trans. Autom. Control, **61**(5), pp. 1391–1396.

[12] Arabi, E., Yucelen, T., and Haddad, W. M., 2017, "Mitigating the Effects of Sensor Uncertainties in Networked Multi-Agent Systems," ASME J. Dyn. Syst. Meas. Control, **139**(4), p. 041003.

[13] Silvestre, D., Rosa, P., Cunha, R., Hespanha, J. P., and Silvestre, C., 2013, "Gossip Average Consensus in a Byzantine Environment Using Stochastic Set-Valued Observers," 52nd IEEE Conference on Decision and Control, Florence, Italy, Dec. 10–13, pp. 4373–4378.

[14] Silvestre, D., Rosa, P., Hespanha, J. P., and Silvestre, C., 2014, "Finite-Time Average Consensus in a Byzantine Environment Using Set-Valued Observers," American Control Conference, Portland, OR, June 4–6, pp. 3023–3028.

[15] Valcher, M. E., and Misra, P., 2014, "On the Consensus and Bipartite Consensus in High-Order Multi-Agent Dynamical Systems With Antagonistic Interactions," Syst. Control Lett., **66**, pp. 94–103.

[16] Hengster-Movric, K., You, K., Lewis, F. L., and Xie, L., 2013, "Synchronization of Discrete-Time Multi-Agent Systems on Graphs Using Riccati Design," Automatica, **49**(2), pp. 414–423.

[17] Zhang, H., Lewis, F. L., and Das, A., 2011, "Optimal Design for Synchronization of Cooperative Systems: State Feedback, Observer and Output Feedback," IEEE Trans. Autom. Control, **56**(8), pp. 1948–1952.

[18] Peng, Z., Wang, D., Zhang, H., Sun, G., and Wang, H., 2013, "Distributed Model Reference Adaptive Control for Cooperative Tracking of Uncertain Dynamical Multi-Agent Systems," IET Control Theory Appl., **7**(8), pp. 1079–1087.

[19] Anderson, B. D., and Moore, J. B., 1979, *Optimal Filtering*, Prentice Hall, Englewood Cliffs, NJ.

[20] Polyak, B. T., Nazin, S. A., Durieu, C., and Walter, E., 2004, "Ellipsoidal Parameter or State Estimation Under Model Uncertainty," Automatica, **40**(7), pp. 1171–1179.

[21] Chabane, S. B., Maniu, C. S., Alamo, T., Camacho, E. F., and Dumur, D., 2014, "A New Approach for Guaranteed Ellipsoidal State Estimation," IFAC Proc. Vol., **47**(3), pp. 6533–6538.

[22] Shamma, J. S., and Tu, K.-Y., 1997, "Approximate Set-Valued Observers for Nonlinear Systems," IEEE Trans. Autom. Control, **42**(5), pp. 648–658.

[23] El Ghaoui, L., and Calafiore, G., 2001, "Robust Filtering for Discrete-Time Systems With Bounded Noise and Parametric Uncertainty," IEEE Trans. Autom. Control, **46**(7), pp. 1084–1089.

[24] Yang, F., and Li, Y., 2009, "Set-Membership Filtering for Discrete-Time Systems With Nonlinear Equality Constraints," IEEE Trans. Autom. Control, **54**(10), pp. 2480–2486.

[25] Yang, F., and Li, Y., 2009, "Set-Membership Filtering for Systems With Sensor Saturation," Automatica, **45**(8), pp. 1896–1902.

[26] Wei, G., Liu, S., Song, Y., and Liu, Y., 2015, "Probability-Guaranteed Set-Membership Filtering for Systems With Incomplete Measurements," Automatica, **60**, pp. 12–16.

[27] Xiao, F., and Wang, L., 2012, "Asynchronous Rendezvous Analysis Via Set-Valued Consensus Theory," SIAM J. Control Optim., **50**(1), pp. 196–221.

[28] Munz, U., Papachristodoulou, A., and Allgower, F., 2012, "Delay Robustness in Non-Identical Multi-Agent Systems," IEEE Trans. Autom. Control, **57**(6), pp. 1597–1603.

[29] Garulli, A., and Giannitrapani, A., 2011, "Analysis of Consensus Protocols With Bounded Measurement Errors," Syst. Control Lett., **60**(1), pp. 44–52.

[30] Sadikhov, T., Haddad, W. M., Yucelen, T., and Goebel, R., 2017, "Approximate Consensus of Multiagent Systems With Inaccurate Sensor Measurements," ASME J. Dyn. Syst. Meas. Control, **139**(9), p. 091003.

[31] Ge, X., Han, Q.-L., and Yang, F., 2017, "Event-Based Set-Membership Leader-Following Consensus of Networked Multi-Agent Systems Subject to Limited Communication Resources and Unknown-but-Bounded Noise," IEEE Trans. Ind. Electron., **64**(6), pp. 5045–5054.

[32] Jiang, Z.-P., and Wang, Y., 2001, "Input-to-State Stability for Discrete-Time Nonlinear Systems," Automatica, **37**(6), pp. 857–869.

[33] Lazar, M., Heemels, W. P. M. H., and Teel, A. R., 2013, "Further Input-to-State Stability Subtleties for Discrete-Time Systems," IEEE Trans. Autom. Control, **58**(6), pp. 1609–1613.

[34] Bhattacharjee, D., and Subbarao, K., 2020, "Set-Membership Filter for Discrete-Time Nonlinear Systems Using State Dependent Coefficient Parameterization," eprint arXiv:2001.06562v2.

[35] Vandenberghe, L., and Boyd, S., 1996, "Semidefinite Programming," SIAM Rev., **38**(1), pp. 49–95.

[36] Sontag, E. D., 2003, "A Remark on the Converging-Input Converging-State Property," IEEE Trans. Autom. Control, **48**(2), pp. 313–314.

[37] Löfberg, J., 2004, "Yalmip: A Toolbox for Modeling and Optimization in Matlab," Proceedings of the CACSD Conference, Vol. 3, Taipei, Taiwan, Portland, OR, Sept. 2–4, pp. 284–289.